Scaling Laws for Pulsed Electric Propulsion with Application to the Pluto Express Mission*

J.K. Ziemer†, E.Y. Choueiri‡ and R.G. Jahn§
Electric Propulsion and Plasma Dynamics Laboratory
Princeton University
Princeton, New Jersey 08544

Abstract

A set of universal laws for the scaling of pulsed electric propulsion systems is presented. The Langmuir characteristic velocity and another characteristic velocity defined here as the pulsed electric propulsion (PEP) characteristic velocity are the two governing parameters in these scaling laws. The Langmuir and PEP characteristic velocities describe the relation of the power generator mass and the energy storage system mass to the propellant mass required to perform a given mission. An optimal exhaust velocity that maximizes the useful mass fraction of the spacecraft can be found using these two parameters. This technique especially applies to low power, small spacecraft where the mass of the energy storage system could make up a significant fraction of the total mass. An Ablative Pulsed Plasma Thruster (APPT) is used as an example low power pulsed electric propulsion system applied to the Pluto Express Mission. A 100% increase in the scientific payload mass of a recent probe design is demonstrated by replacing the chemical propulsion system with an optimized APPT system using only well proven off-the-shelf technologies.

1 Introduction

Electric propulsion devices with their large specific impulse values have been studied for numerous applications including satellite stationkeeping, orbit raising, and interplanetary travel[1, 2, 3, 4]. They are different from chemical propulsion systems by being *power* limited; the power supplied to the device directly relates to an increase in exhaust velocity and specific impulse. The ability to supply large amounts of power without demanding massive power supplies becomes important in the overall design. For many currently available power generators, however, the propellant mass saving that can be realized with higher exhaust velocities is offset by the increasing mass of the power supply. In addition, most electric propulsion devices have higher efficiencies at higher power making operation at lower power still costly in terms of power plant mass.

Pulsed electric propulsion (PEP) systems avoid the cost of operating at high power by storing energy and releasing it in a quick pulse. Pulsing allows the thruster to use less power over a longer time while still obtaining the benefits of higher exhaust velocities and efficiencies. The added mass of the energy storage system, however, can be a significant fraction of the total spacecraft mass and must be considered in the spacecraft design as well as the power plant mass.

The Ablative Pulsed Plasma Thruster (APPT) is a pulsed electromagnetic thruster using a fluorinated polymer for propellant. It is the only electric propulsion system proven in space[5, 6] to operate at powers below 100 W. The APPT's simple configuration and easy construction allow a proven empirical method for design[7, 8] while making the system more attractive for long term missions, such as stationkeeping, where reliability is a concern[9, 10, 11].

APPT technology can also be applied to other long term missions such as unmanned interplanetary exploration. NASA's Pluto Express Mission is a low mass, low power mission currently in the design stage. Pluto's distance from the sun and a relatively short mission time constraint require a large change in the probe's kinetic energy. Total cost, including the

*Support from NASA Jet Propulsion Laboratory and the Air Force Office of Scientific Research

†Graduate Student, Department of Mechanical and Aerospace Engineering

‡Chief Scientist and Lab Manager, Member AIAA

§Professor, Department of Mechanical and Aerospace Engineering, Fellow AIAA launching system, is also a primary driver in the design. Currently, a large launch system such as the Titan IV or Proton is being considered by NASA although these systems are expensive. Electric propulsion options have been studied for this mission[12, 13] to reduce the booster size and cost. Almost all proposed designs, whether using electric propulsion or not, have the final leg of the mission (where solar power is not readily available) being completed by a chemical propulsion system with a Radioisotope Thermoelectric Generator (RTG) power supply.

One goal of this paper is to demonstrate the propellant mass savings obtained by choosing an optimized APPT system instead of the proposed chemical system for the Pluto Express Mission. An APPT system is the only electric propulsion device that is technologically developed enough to be used on a mission with such a low amount of power available. In this paper, an optimal APPT system configuration is found by developing *general* pulsed electric propulsion scaling laws that include both the power generator mass and the energy storage system mass. Two characteristic velocities, the Langmuir characteristic velocity and the PEP characteristic velocity, provide a basic approach for optimizing the useful mass fraction of a spacecraft. This method will be applied using APPT technology parameters and the design of an optimized APPT system for the Pluto Express Mission will be presented.

2 Scaling Laws for Pulsed Electric Propulsion Systems

In field-free space, the relation between a change in spacecraft velocity, the mass of propellant expended during the maneuver, and the exhaust velocity of the thruster is given by the rocket equation:

$$\Delta V = \bar{u}_e \ln\left(\frac{1}{1-F}\right), \tag{1}$$

where the change in velocity is ΔV, the average effective exhaust velocity is $\bar{u}_e$, and the propellant mass fraction, M_p/M_0, is F. This analysis will assume an approximate field-free case when the mission characteristic velocity, ΔV, is given. This becomes a poor assumption for long operation times although an effective characteristic velocity can still be meaningful.

This section will develop the mass relations for a spacecraft using PEP technology and present two characteristic velocities that can be used to optimize the useful mass fraction of the spacecraft. A closed-form approximation of the optimal exhaust velocity is also presented. A non-dimensional formation of the model with parameters that govern the scaling of the relevant system masses is constructed. Finally, parametric sensitivity in this model is discussed. This analysis will form the basis of a universal description that can be used for any pulsed electric propulsion system.

2.1 Mass Equations

The total mass of a spacecraft using electric propulsion can be formulated as:

$$M_0 = M_u + M_s + M_g + M_a + M_p + M_t, \tag{2}$$

where M_0 is the total initial mass, M_u is the useful mass, M_s is the structural mass, M_g is the power generator mass, M_a is the accelerator or thruster mass, M_p is the propellant mass, and M_t is the propellant tank mass.

This expression can be reduced to fewer unknown variables by the following relations. The structural mass can be considered proportional to the initial total mass by a structural constant, $M_s = K_s M_0$. Similarly, the propellant tank mass can be considered proportional to the propellant mass, $M_t = K_t M_p$. The mass of the power generator is the sum of an initial mass regardless of power level, M_{gfix}, and a power-dependent mass, $K_g P_{ga}$, where K_g is the specific mass of the power supply and P_{ga} is the power available from the power supply for the propulsion system. In the case of a PEP system, the thruster mass is given by:

$$M_a = M_{afix} + M_{as} + M_{apc} + M_{aes}, \tag{3}$$

where M_a is the total thruster mass. M_{afix} is a fixed mass made up of the power-independent part of the power conditioning system and the size-independent parts of the thruster. This includes the electrodes and discharge initiation circuitry. M_{as} is the thruster structural mass, M_{apc} is the power conditioner mass, and M_{aes} is the energy storage system mass.

Again, some simplification can occur by using proportionality relations. The structural mass should be proportional to the total thruster mass, $M_{as} = K_{as} M_a$. The power conditioning system mass with a specific mass of K_{apc} will follow a similar relation to the available power as the power generator mass described previously, $M_{apc} = K_{apc} P_{ga}$. Finally, the energy storage system mass will be proportional to the energy stored in the system, E, $M_{aes} = K_{aes} E$.

Combining some of the specific mass constants for available power and energy, $\alpha_g = K_g + K_{apc}/(1 - K_{as})$,

$\alpha_a = K_{aes}/(1-K_{as})$, and adding the fixed masses together, $M_x = M_{gfix} + M_{afix}/(1-K_{as})$, equation 2 becomes:

$$M_0 = M_u + K_s M_0 + M_x + \alpha_g P_{ga} + \alpha_a E + M_p(1+K_t). \quad (4)$$

Dividing by the initial total mass, M_0, and introducing mass fraction notation:

$$1 = U + K_s + X + G + A + F(1+K_t), \quad (5)$$

where U is the useful mass fraction, X is the fixed mass fraction, G is the power system mass fraction, A is the thruster mass fraction, and F is the propellant mass fraction as noted previously.

2.2 Characteristic Velocities

As developed by Langmuir[1], a single characteristic velocity can describe the relation between the power system mass fraction and the propellant mass fraction. A similar method can also be used to find another characteristic velocity describing the PEP system mass fraction. Both of these velocities require the definition of a characteristic mission time. Let τ be the total operation time that the thruster is activated and drawing power. During this time, the thruster will be pulsing at its maximum frequency f_{max} for a total of N_{ptot} pulses:

$$f_{max} = N_{ptot}/\tau. \quad (6)$$

The mass flow rate and mass bit can now be defined as follows:

$$\dot{m} = f_{max} m_{bit} = \frac{M_p}{\tau}, \quad (7)$$

$$m_{bit} = \frac{M_p}{N_{ptot}}. \quad (8)$$

The actual power and energy in the exhaust are related to the supplied power and energy by the following efficiency equations:

$$\eta P_{ga} = \frac{1}{2}\dot{m}\bar{u}_e^2, \quad (9)$$

$$\eta_a E = \frac{1}{2} m_{bit}\bar{u}_e^2, \quad (10)$$

where η, the total efficiency, is defined as the product of the power conditioner efficiency, η_{pc}, and the thruster efficiency, η_a, $\eta = \eta_{pc}\eta_a$. Define two characteristic velocities, the Langmuir characteristic velocity and the PEP characteristic velocity:

$$\tilde{U} \equiv \sqrt{\frac{2\eta\tau}{\alpha_g}}, \quad (11)$$

$$\tilde{V} \equiv \sqrt{\frac{2\eta_a N_{ptot}}{\alpha_a}}. \quad (12)$$

By substituting equations 7, 8, 11, and 12 into equations 9 and 10, the following relations between mass fractions are produced:

$$G = F(\frac{\bar{u}_e}{\tilde{U}})^2, \quad (13)$$

$$A = F(\frac{\bar{u}_e}{\tilde{V}})^2. \quad (14)$$

Equation 5 now simplifies to:

$$1 = U + K_s + X + F\left(1 + K_t + (\frac{\bar{u}_e}{\tilde{U}})^2 + (\frac{\bar{u}_e}{\tilde{V}})^2\right). \quad (15)$$

Using a modified form of the rocket equation, eq. 1, a final equation for the useful mass fraction becomes:

$$U = 1 - K_s - X - (1 - e^{-\Delta V/\bar{u}_e})\left(1 + K_t + (\tfrac{\bar{u}_e}{\tilde{U}})^2 + (\tfrac{\bar{u}_e}{\tilde{V}})^2\right). \quad (16)$$

The useful mass fraction is dependent on three known constants: K_s, K_t, and X and four velocities: ΔV, $\bar{u}_e$, $\tilde{U}$, and $\tilde{V}$. Of the four velocities, one is given by the mission parameters, ΔV. Two are based on thruster technology, operation time, and the power generator specific mass, $\tilde{U}$ and $\tilde{V}$. Finally, the exhaust velocity, $\bar{u}_e$, is a free parameter used to optimize the useful mass fraction.

2.3 Optimization, Scaling Laws, and Parametric Sensitivity

An approximate optimal exhaust velocity in closed-form can be found with two assumptions. First, the Langmuir and PEP characteristic velocities are assumed to be independent of the exhaust velocity (the thruster efficiency cannot be a function of the exhaust velocity.) Second, the exhaust velocity is assumed to be much larger than the mission ΔV.

$$\frac{\partial \tilde{U}}{\partial \bar{u}_e} = \frac{\partial \tilde{V}}{\partial \bar{u}_e} = 0, \quad (17)$$

$$\bar{u}_e \gg \Delta V. \quad (18)$$

The optimal exhaust velocity can now be described by the following relation:

$$\frac{1}{\bar{u}_e^2} = \frac{1}{\tilde{U}^2} + \frac{1}{\tilde{V}^2}. \quad (19)$$

This relation is obtained by taking the derivative of the useful mass fraction with respect to the exhaust velocity. The exponential function is expressed in a Taylor series keeping only the zero and first order terms, while all "small" terms ($1/n^3$ and K_t) are dropped. This leaves a simple description for the optimal exhaust velocity that is *not* dependent on the mission ΔV.

Unfortunately, the efficiency and, therefore, the two characteristic velocities are typically functions of the exhaust velocity. In that case, this relation is no longer true. Equation 19, however, is still useful as an approximation, and helpful to see general trends in the optimization problem.

It is apparent through equations 16 and 19 that larger Langmuir and PEP characteristic velocities yield higher useful mass fractions and higher optimal exhaust velocities. For the Langmuir characteristic velocity, increasing the operation time, increasing the efficiency, or decreasing the specific mass of the power system can have the *same* beneficial result. Similarly, equal changes in the number of total pulses, the thruster efficiency, or the specific mass of the energy storage system can all impact the PEP characteristic velocity in the same way. Figures 1 and 2 show the relations between the characteristic velocities and the useful mass fraction with the introduction of a propulsion parameter, Γ, that defines a universal set of non-dimensional scaling laws:

$$\Gamma = 1 + \left(\frac{\bar{u}_e}{\tilde{U}}\right)^2 + \left(\frac{\bar{u}_e}{\tilde{V}}\right)^2, \tag{20}$$

$$\Gamma = \frac{1 - U - K_s - X}{1 - e^{-\Delta V/\bar{u}_e}} - K_t. \tag{21}$$

By using equations 1 and 4 the propulsion parameter can be understood as the ratio of the power system, thruster and propellant mass to the propellant mass,

$$\Gamma = \frac{\alpha_g P_{ga} + \alpha_a E + M_p}{M_p}. \tag{22}$$

A small propulsion parameter, of first order, would indicate that the masses of the power system and thruster are on the same order as the propellant mass required to perform the ΔV maneuver. A large Γ would indicate a massive power system or thruster compared to the propellant mass.

As seen in figure 1, smaller Γ values relate to smaller non-dimensional characteristic velocities, $\bar{u}_e/\tilde{U}$ and $\bar{u}_e/\tilde{V}$. This is true of a system with *larger* Langmuir and PEP characteristic velocities and *smaller* exhaust velocities. Figure 2, however, shows that larger exhaust velocities relate to larger useful mass fractions for a given ΔV. This conflict

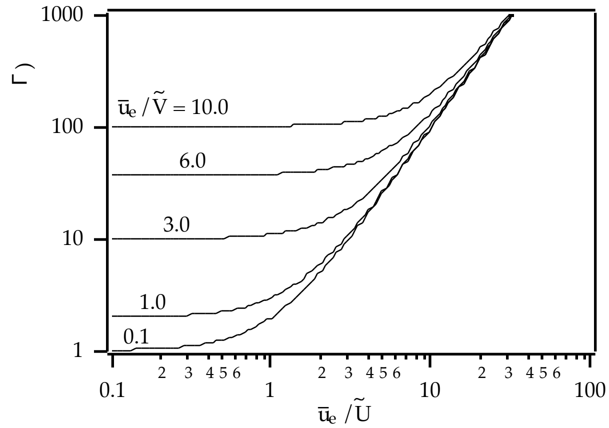

Figure 1: Propulsion parameter Γ as a function of the Langmuir and PEP characteristic velocities non-dimensionalized by the exhaust velocity as described by eq. 20.

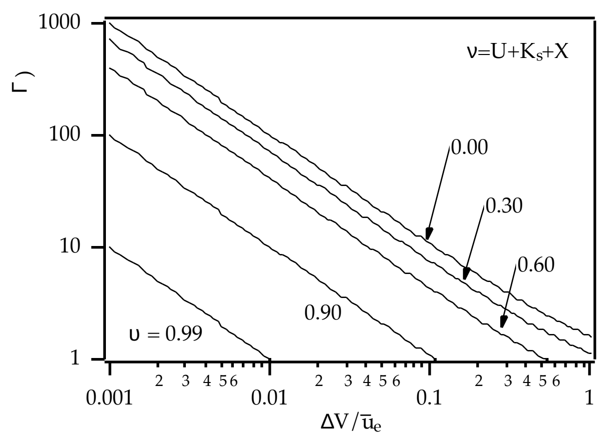

Figure 2: Propulsion parameter Γ as a function of the mission characteristic velocity non-dimensionalized by the exhaust velocity with varying power-independent mass fraction constants, ν. This figure is described by eq. 21 with the assumption that K_t is negligible compared to ν.

points to an optimal exhaust velocity that will maximize the useful mass fraction while keeping $\bar{u}_e/\tilde{U}$ and $\bar{u}_e/\tilde{V}$ within reasonable bounds.

Figure 3 shows that the useful mass fraction can be maximized with the choice of an optimal exhaust velocity. For fixed Langmuir and PEP characteristic velocities, the optimal exhaust velocity for a maximum useful mass fraction will follow equation 19. Figure 4 shows this relation for typical small mass, low power mission ranges of the Langmuir and PEP characteristic velocities. Both characteristic velocities affect the maximum useful mass fraction and optimal exhaust velocity in the same way. If the two velocities are not of the same magnitude, only the smaller of the two will have an impact on the optimization. The optimal exhaust velocity will, therefore, always be near the same order of magnitude as the smallest characteristic velocity. This leads to optimal propulsion parameters *always* being close to one. The optimal propulsion parameter can increase, however with the increasing optimal exhaust velocities that come from including efficiency as a function of exhaust velocity.

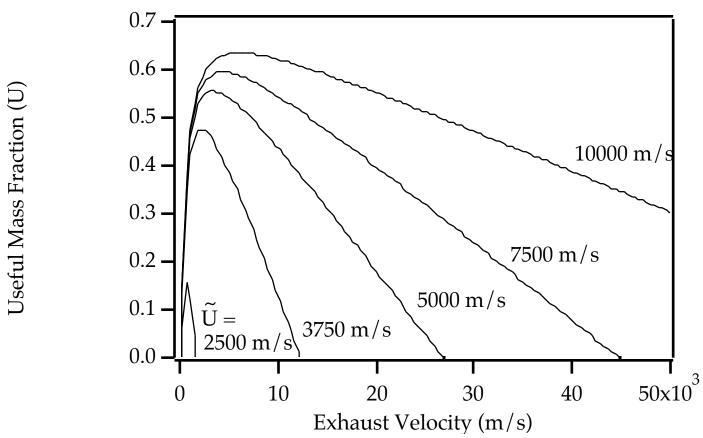

Figure 3: Useful mass fraction as a function of exhaust velocity with varying Langmuir characteristic velocity values. Approximate parameters are taken from the Pluto Express Mission with an APPT system: $\tilde{V}$ = 12 km/s, ΔV = 350 m/s, K_s = 0.13, X = 0.13, and K_t=0.

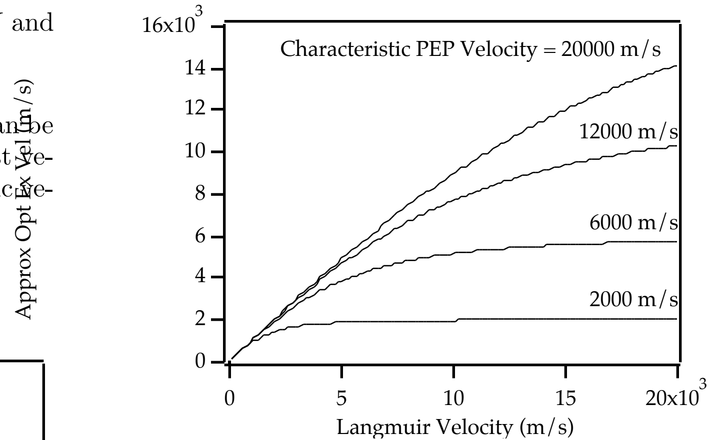

Figure 4: Optimal exhaust velocities for typical ranges of Langmuir and PEP characteristic velocities from equation 19.

3 Scaling Laws Applied to APPT Systems

An Ablative Pulsed Plasma Thruster is an example PEP system already used in space. The APPT is an electromagnetic accelerator that typically uses a capacitor for its energy storage system. On flight-ready models, the LES 8/9 micropound thrust APPT[5] and the AFRPL millipound thrust APPT[14] for example, power consumption is below 150 Watts, the specific impulse has been measured between 200 and 2000 sec., and the efficiencies have reached up to 50%[5, 10, 15, 16]. Using modern capacitor and power conditioner technology data, (an effort is made to use only existing technology and data values that have been used in previous mission studies and verified empirically) the PEP characteristic velocity can be calculated for a given efficiency. Efficiency has been shown, however, to be a function of the exhaust velocity[10, 16] and this significantly affects the PEP characteristic velocity for optimization purposes.

In this section, the values for the specific mass parameters outlined in section 2.1 along with two models for the exhaust velocity dependent efficiency will be presented.

3.1 Capacitor Technology

Capacitor technology has improved a great deal over the last decades[17]. Electrostatic film capacitors seem to show the most promise for this application[17, 18]. Their specific mass ranges from 0.1 - 0.01 kg/J and they have documented laboratory lifetimes of $10^6 - 10^8$ pulses[17, 19]. Previous APPTs have used oil impregnated aluminum foil-mylar-paper layers and a polyvinylidene fluoride (PVDF) capacitor film with respective specific masses of 0.045 kg/J and 0.011 kg/J and pulse lifetimes on the order of 10^7 and 10^6 pulses. From observing the data, there appears to be a trade-off between specific mass and pulse lifetime. The specific mass magnitude does not appear to vary as much as the total pulse lifetime magnitude, however, and both can be seen to affect the PEP characteristic velocity in the same way (see eq. 12.) For this reason, capacitors with higher pulse lifetimes and *higher* specific masses may be favorable. A higher pulse rate and lower pulse energy follow with the choice of a long pulse lifetime capacitor. Ennis[19] reports that rapid rate capacitors with a 0.064 kg/J specific mass and a 10^{10} pulse lifetime have been built. This technology is still under development, and applications for the APPT are, unfortunately, not yet available. Rather, another alternative that can be considered "off-the-shelf" technology, ceramic capacitors, will be adopted for this study. With a specific mass near 0.02 kg/J and a lifetime predicted above 10^7 pulses, this technology is well suited for the APPT. This type of capacitor, or at least, specific mass and pulse lifetime values that are close to this capacitor have been used in other APPT mission studies[10, 11, 20], and they will be used here as well.

3.2 Power Conditioner Technology

Power conditioner technology, unlike capacitor technology, has not changed a great deal over the past years. Dethlefsen and Ennis[17] describe a high power design that operates at 93.5% efficiency with a specific mass of 4.4 kg/kW. In Guman's paper on designing APPT systems[8], suggested values for efficiency and specific mass are 80% and 11 kg/kW, respectively, with a 0.5 kg power-independent fixed mass for systems operating below 200 Watts. These values will be used in this study, and again, similar values have been used previously[10, 20].

3.3 Structural and Propellant Tank Specific Mass

For the LES 8/9 APPT and the AFRPL millipound APPT, the mass of the structure alone makes up approximately ten percent of the total thruster mass without the propellant or propellant storage system included[8, 21]. Yet the propellant tank mass does not make up a significant part of the total probe mass since the solid Teflon propellant does not need to be stored in a pressurized tank. Instead, the tank mass and the propellant feeding system mass can be incorporated into the structural mass of the thruster. For this study, the parameters in question are set as follows: $K_t = 0$ and $K_{as} = 0.2$. Other sources besides Fairchild Industries also approximated the structural mass by 20% of the total thruster mass including the propellant tank mass[10].

3.4 Fixed Mass

The fixed mass is made up of the power-independent mass of the power conditioning system, the electrode mass, and the discharge circuitry mass. Again, using Guman's paper on APPT design along with other sources that confirm the approximations[8, 5, 21], the values used in this analysis are as follows: 0.5 kg fixed power conditioner mass, 1 kg electrode mass, 0.2 kg discharge initiation circuitry mass, and a total fixed thruster mass, M_{afix}, equal to 1.7 kg. These values are derived from an APPT with a discharge energy of approximately 200 J and an expected lifetime of 10^7 pulses. The mass of the electrodes could be significantly reduced for designs that have lower discharge energies,require fewer pulses to complete the mission, or are made of a different material[22, 23]. The power-independent part of the power conditioner mass and the discharge circuitry mass do not change significantly with discharge energy.

3.5 Efficiency Models

In order to design APPT thrusters, empirical models that predict mass ablation rates depending on electrode geometry and discharge energy have been created. The discharge energy, E, divided by the impulse bit, I_{bit}, has been shown to be an important scaling parameter in this mass ablation function:

$$\varepsilon \equiv \frac{E}{I_{bit}}. \tag{23}$$

The mass ablation relation is stated as follows:

$$F(\varepsilon) = \frac{m_{bit}}{E}. \tag{24}$$

Using this function, the exhaust velocity and thruster efficiency can be expressed as:

$$\bar{u}_e = \frac{I_{bit}}{m_{bit}} = \frac{1}{F(\varepsilon)\varepsilon}, \tag{25}$$

$$\eta_a = \frac{\frac{1}{2} m_{bit} \bar{u}_e^2}{E} = \frac{F(\varepsilon)\bar{u}_e^2}{2}. \tag{26}$$

The exhaust velocity and efficiency can now be seen to be functions of ε alone with the inclusion of the mass ablation function.

Two separate relations for the mass ablation function have been suggested by Fairchild Industries[16] and the RIAME of the Moscow Aviation Institute in Russia[10]. Fairchild bases their function on data from the AFRPL millipound thrust APPT with a side-fed propellant geometry,

$$F(\varepsilon) = 1320\,\varepsilon^{-8/3}. \tag{27}$$

Although the Russian paper does not explicitly state what geometry was used for the ablation function, it falls somewhere between known the side-fed AFRPL millipound APPT and the breech-fed LES 8/9 APPT,

$$F(\varepsilon) = 6.25 \times 10^9\,\varepsilon^{-4}. \tag{28}$$

Figure 5 shows a graphical representation of the two ablation functions and data points from the two well studied systems along with a generated data fit for breech-fed thrusters. It is interesting to note that

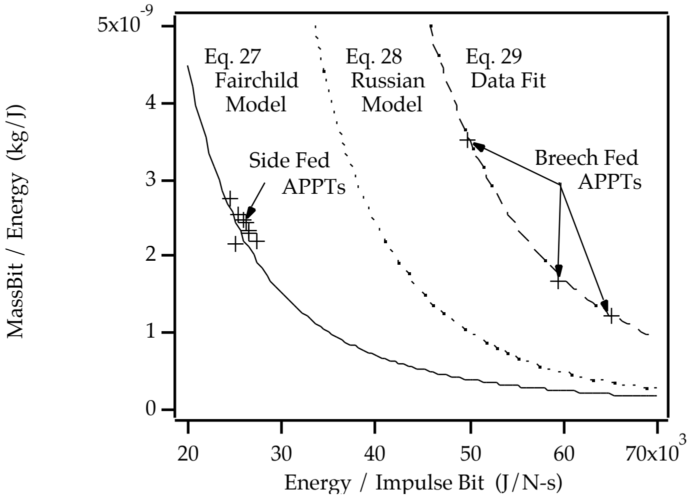

Figure 5: Ablation models for breech-fed and side-fed APPT geometries with APPT system data [5, 8, 21].

with a modification of the coefficient on the Russian ablation function, the breech-fed data points are well predicted:

$$F(\varepsilon) = 22 \times 10^9\,\varepsilon^{-4}. \tag{29}$$

This modified function will not be used, however, in this study.

Using equations 25 and 26 along with the ablation functions, eq. 27 and 28, efficiency can be expressed as a function of exhaust velocity. The Fairchild model predicts,

$$\eta_a = 6.71 \times 10^{-3}\,\bar{u}_e^{2/5}, \tag{30}$$

while the Russian model predicts a slightly lower value,

$$\eta_a = 271 \times 10^{-6}\,\bar{u}_e^{2/3}. \tag{31}$$

These two efficiency relations are compared in figure 6. The more conservative Russian model will be

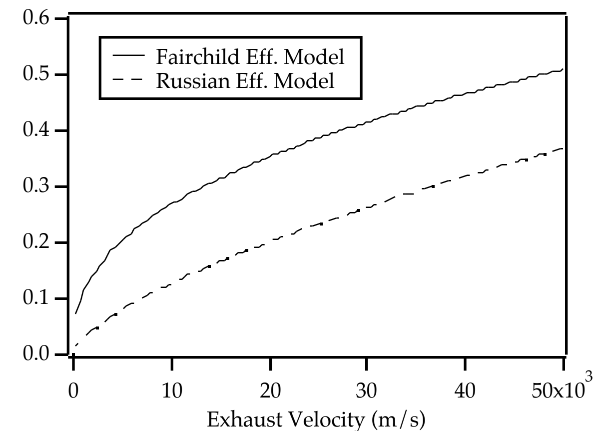

Figure 6: Efficiency as a function of exhaust velocity for the two different ablation models.

used in this paper for the example Pluto Express Mission.

3.6 Summary of APPT Parameters and Discussion of Characteristic Velocities

A summary of values discussed for APPT systems is presented in table 1. With these values and thruster efficiencies ranging from 5-40%, the PEP characteristic velocity can vary between 7-20 km/s. Using a thruster efficiency near 20% gives a reasonable PEP characteristic velocity example, $\tilde{V}$=12.6 km/s, for estimating the optimal exhaust velocity. It is important to realize that since the PEP characteristic velocity is on the same order as typical exhaust velocities from APPT systems, the thruster and energy storage system should make up a significant fraction of the total

Cap. Spec. Mass	K_{aes}	=	0.02 kg/J
Cap. Lifetime	N_{ptot}	=	10^7 Pulses
P. Cond. Spec. Mass	K_{apc}	=	11 kg/kW
P. Cond. Efficiency	η_{pc}	=	0.80
Structural Mass Frac.	K_{as}	=	0.20
Fixed Mass	M_{afix}	=	1.7 kg
APPT Spec. Mass	α_a	=	0.025 kg/J
Approx. PEP Vel. (20% Thruster Eff.)	$\tilde{V}$	=	12.6 km/s

Table 1: Summary of APPT parameters.

mass compared to the propellant mass as discussed in section 2.3.

The Langmuir characteristic velocity is more of a mission dependent parameter. Still, order of magnitude estimates can be made by using reasonable values for operating time, efficiency, and the power generator specific mass. For stationkeeping missions where operation times can be on the order of ten years and solar power is typically used, the Langmuir characteristic velocity is quite high. Using 30 kg/kW as a reasonable power plant specific mass[24] and a *total* efficiency of 16%, the Langmuir characteristic velocity would be approximately 58 km/s, significantly higher than the PEP characteristic velocity for an APPT system. This indicates that the power supply necessary to run the APPT would be less massive than the energy storage system. The approximation for the optimal exhaust velocity, eq. 19, predicts $\bar{u}_e$=13.5 km/s using the largest possible characteristic velocities. Figures 1 and 2 can now be used to determine the propulsion parameter and power-independent mass fraction depending on the mission ΔV. Typically, on board most earth bound satellites, the power supply would mainly be used for payload devices and only a small fraction would need to be dedicated to the thrusters.

For orbit raising missions where operation time is an important concern, the Langmuir characteristic velocity can become much smaller. Using a similar solar power generator with a single month to perform the mission, the Langmuir characteristic velocity drops an order of magnitude to 5 km/s. It should also be noted that for the case of a large spacecraft or, in general, where kilowatts of power are required to perform the maneuver, other electric propulsion systems with higher efficiencies may be better suited to the task. An example of a mission where APPT systems are indeed the best choice would be small satellite orbit raising missions. These spacecraft are becoming more popular having masses near 100 kg requiring a smaller and cheaper launch vehicle. The power supply will have a reduced specific mass near 10 kg/kW and probably be supplying less than a kilowatt total[25]. APPT systems are one of the only electric propulsion technologies that have demonstrated operation at those low powers[26].

Interplanetary missions can also be considered. Although mission times are long enough to have large Langmuir characteristic velocities, larger probes or missions with large ΔV requirements will necessitate high exhaust velocities for decent useful mass fractions (see fig. 2.) This, again, points to bigger power supplies and other, more efficient electric propulsion systems. For small mass and low power spacecraft that only require small changes in velocity, however, an APPT system can be a viable alternative. The Pluto Express Mission is a good example of this type of spacecraft.

4 The Pluto Express Mission

Pluto is the only planet yet to be investigated by an unmanned probe. Recent observations showing the existence of an atmosphere around Pluto have led to an interest in finally exploring the last planet in our solar system by the year 2020 when the atmosphere could be frozen to the surface[27, 28]. Studying Pluto's atmosphere, geology, and surface composition could give some answers about the outer solar system origin and composition. These questions form the basis for the scientific goals of the Pluto Mission.

The Pluto Express Mission will require a small probe on a fast fly-by trajectory, either ballistic or with minimal gravity assists, to reach the planet in time while using an available launcher and keeping costs down. For the ballistic case, the probe itself will be small and a large, expensive launching system, possibly a Proton or Titan IV, will be used to provide the solar escape energy. Another possibility would be to use either gravity assist maneuvers, a SEP booster stage, or a combination of the two to reduce the size and expense of the launcher with the trade-off of added mission duration. In either trajectory type, the final stage of the mission will consist of a low mass probe with limited power resources.

During the mission, the main propulsion system will be required to perform trajectory correction maneuvers while the reaction control system (RCS) keeps the spacecraft oriented. The propellant and the support mass (tankage, pipes, valves, etc.) is ex-

Mass Allocations:	(kg)	(frac)
Power Subsystem	19.4	0.17
Structure	14.6	0.13
Propulsion	9.9	0.09
Useful Mass:	(36.6)	(0.32)
Telecommunications	12.8	0.11
Attitude Control	6.6	0.06
Spacecraft Data	6.5	0.06
Thermal Control	3.7	0.03
Science Payload	7.0	0.06
Dry Mass:	80.5	0.71
Contingency (20%)	16.1	0.14
Propellant (ΔV=350 m/s)	17.0	0.15
Total Mass:	**113.6**	**1.00**

Table 2: 1993 Pluto Express design mass distribution.

pected to make up a significant portion of the total probe mass for a chemical system. Table 2 shows the mass breakdown of a recently published design for the Pluto Express Mission[28]. For this study, the ΔV supplied by the propulsion system during the mission is assumed to be 350 m/s with a dry mass contingency of 20%. This section of the paper will describe the propulsion and power systems used in the recent Pluto Express design.

4.1 Propulsion System

One propulsion system proposed for this mission is described in ref. [29]. It consists of a hybrid monopropellant hydrazine blow-down design pressurized with nitrogen that will also be used for the cold gas RCS. The system design is fully redundant with at least one duplicate component for each important part: the valves and thrusters. The cold gas thrusters, the latch valves, and the regulators are all derivatives of the Strategic Defense Initiative program with very small masses and long lifetimes that are expected to be greater than 10 years. Newer designs may have slight changes, however, only published design information is used in this study.

The main ΔV propulsion system consists of three 4.4 N hydrazine thrusters providing 15 N of total thrust while using 22 W of power during peak periods of operation and less than 3 W during normal operation. The thrusters have an I_{sp} of 220 s and, in this design, have enough propellant to deliver a Delta V equal to 350 m/s.

The RCS is made up of eight 4.5×10^{-3} N nitrogen cold gas thrusters that each have an I_{sp} of 57 s. The minimum impulse bit required for each thruster is less than 1×10^{-4} N-s with a total mission impulse of 250 N-s supplied by about half a kilogram of nitrogen propellant.

Subsystem:	Power (W)
Telecommunications	9.0
Attitude Control	9.9
Data Processing	8.6
Power Conditioning	15.1
Thermal Control	1.0
Science Payload	1.0
Total Power:	**44.6**

Table 3: 1993 Pluto Express design power consumption in cruise phase.

The total propulsion system mass including the nitrogen propellant for the RCS but not the hydrazine propellant for the ΔV thrusters is 9.9 kg. The power allotted during propulsion maneuvers is approximately 17 W for opening and holding valves.

4.2 Power System

A Radioisotope Thermoelectric Generator (RTG) is the proposed power generator for the Pluto Express Mission. Other systems have been studied: solar power is not feasible in the outer solar system and other nuclear or battery sources are not yet developed enough to be considered. Schock[30, 31] describes the Pluto Express power system along with modifications of the design to meet mission specifications. The power requirements (not including the power for the propulsion system) during a cruise phase of the mission are presented in table 3.

Like all power systems, the RTG has a power-independent mass that consists of mounting hardware, casing, electrical wiring, etc. After the initial mass, the power output and total mass of the RTG is based on the number of General Purpose Heat Source (GPHS) modules there are, the quality of the plutonium fuel, and the method of power conversion. GPHS modules degrade with time. Assuming that all required power must be available at the “End of Mission” (EOM) date, the EOM power can be used to design the power supply. In addition, a power margin and contingency must be part of the design in case of partial failure or unpredicted power loses.

Currently a variety of power conversion technologies and fuel sources are available. Low power DIPS have been shown to have higher efficiencies and use less plutonium to produce relatively the same amount of power as an RTG[32]. It's initial mass is more than an RTG system, however, and the specific mass for lower powers can be larger than RTG systems. An AMTEC system is another alternative, although it has not yet been proven for use with GPHS modules[33]. Proven GPHS-RTGs using SiGe unicouples have been chosen for the recent Pluto Express design and have been used in many interplanetary missions before[34, 35, 36]. MOD-RTGs using SiGe multi-couples have also been studied for their lower specific mass although the technology is not as well tested as GPHS-RTGs[37].

The plutonium in the heat sources is very expensive. Previously built spare sources are being considered for the Pluto Express Mission to keep costs down. Using Russian plutonium for the heat source results in the lowest specific mass and highest EOM power over using either a Cassini or Galileo spare[30]. With modifications, however, the Galileo or Cassini spare can be made to work for this mission with the power margin and contingency included[31].

5 Using APPT Technology for the Pluto Express Mission

Significant benefits in propellant mass savings can be achieved by switching to a system with a higher exhaust velocity while using approximately the same amount of power. An APPT system can accomplish these savings allowing more payload mass and a demonstration of electric propulsion technology for a mass-critical, low power mission. In this section of the paper, the universal scaling laws previously described will be used to optimize the useful mass fraction. Parameters for the optimization will come from current technology and already tested APPT systems.

5.1 Mission Parameters

A summary of the APPT parameters used for this mission may be seen in table 1. The remaining parameters left to specify are the initial total mass of the probe, the structural mass fraction of the probe, the mission operation time, and the power generator specific mass and fixed mass. Similar to the recent Pluto Express design, the total initial mass will be set at 115 kg and the structural mass fraction will be set to 0.13. The entire mission is projected to last between seven and ten years. For course correction, a long operation time was assumed at a little over two years, or 7×10^7 seconds. This assumption will be discussed in more detail later along with alternative operation times and their impact on the maximum useful mass fraction.

The power supply is assumed to be an GPHS-RTG similar in performance to the devices made for the Cassini mission. The power-independent mass is 4.3 kg. Each module has a mass of 2.3 kg and produces 13 W of power giving a specific mass K_g=0.18 kg/W. As an added constraint, the fixed mass of the power generator will also include supplying enough power to the other subsystems on-board at the same time (see table 3.) The fixed mass for the power generator is, therefore:

$$M_{gfix} = 4.3\,\text{kg} + 44.6\,\text{W} \times 0.18\,\text{kg/W} = 12.3\,\text{kg}. \quad (32)$$

The total fixed mass, fixed mass fraction, and total power generator specific mass can be calculated from the formulas in section 2.1, $M_x = 14.4$ kg, $X = 0.13$, and $\alpha_g = 0.19$ kg/W. A summary of mission parameters for the Pluto Express example is provided in table 4.

Total Init. Mass	M_0	=	115.0 kg
Struc. Mass Frac.	K_s	=	0.13
Fixed Mass Frac.	X	=	0.13
P. Gen. Fixed Mass	M_{gfix}	=	12.3 kg
P. Gen. Spec. Mass	K_g	=	0.18 kg/W
Total P. Spec. Mass	α_g	=	0.19 kg/W
Operation Time	τ	=	7×10^7 s
Approx. Lang. Vel. (20% Thruster Eff.)	$\tilde{U}$	=	10.9 km/s

Table 4: Summary of Pluto Express Mission parameters.

5.2 Characteristic Velocities

Using 20% for an estimate of thruster efficiency and the parameters discussed above, the PEP and Langmuir characteristic velocities are 12.6 km/s and 10.9 km/s, respectively. These values predict an optimum exhaust velocity near 8.2 km/s. However, using the Fairchild and Russian efficiency models, the optimum exhaust velocities are higher at 12.6 km/s and 11.4 km/s, respectively. With the inclusion of the efficiency models, a higher exhaust velocity will lead to higher efficiencies and a slightly higher useful mass fraction can be obtained. The maximum useful mass fractions for the Fairchild and Russian models are 0.67 and 0.63, respectively. The conservative lower values from the Russian model will be adopted in this study.

One assumption that could be called into question is the long operation time for a course correction maneuver. The operation time only affects the Langmuir characteristic velocity directly. Figure 5.2 shows how the optimal exhaust velocity and the maximum useful mass fraction change as a function of operation time for both efficiency models. The time in the graph

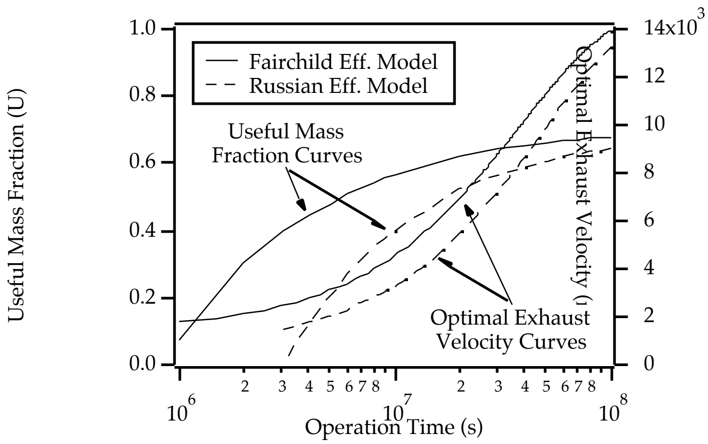

Figure 7: Maximum useful mass fraction and optimal exhaust velocity as a function of operation time. Both the Fairchild and Russian efficiency models are shown.

stretches from 11 days to about 3 years. Notice that even for periods on the order of 100 days (10^7 s) the maximum useful mass fraction is at least above 40%; a value which is higher than the recent design used in this study (see table 2.) Figure 3 also shows how the useful mass fraction changes with varying Langmuir and exhaust velocities for this mission. The two year operating time was chosen to show the importance of the PEP characteristic velocity and to keep the APPT design for this mission close to other already proven designs. A completely realistic and feasible system could be built with present technology, however, at any of the exhaust velocities and efficiencies suggested by this paper.

5.3 APPT System Design

Using the Russian efficiency model and the two year operation time, the optimal exhaust velocity is 11.4 km/s, the PEP characteristic velocity is 10.5 km/s, the Langmuir characteristic velocity is 9.0 km/s, the efficiency is 13.7%, and the maximum useful mass fraction, including contingency and RCS system, is 62.5%. The fuel fraction is 0.03 and the required power for the propulsion system is only 29.5 W. This power along with the other components 44.6 W can be supplied with a 20% contingency at EOM by a seven module Cassini-like RTG.

The main APPT system design is very similar but slightly smaller than the Fairchild millipound APPT. Important parameters for the optimal APPT design can be seen in table 5. The RCS system is made

Fixed Mass	M_{afix}	=	1.7 kg
Struc. Mass	M_{as}	=	1.3 kg
Power Cond. Mass	M_{apc}	=	0.3 kg
Capacitor Mass	M_{aes}	=	3.3 kg
Total Mass	M_a	=	6.6 kg
Power Requirement	P_{ga}	=	29.5 W
Discharge Energy	E	=	164 J
Pulse Frequency	f	=	0.14 Hz
Mass Bit	m_{bit}	=	0.35 mg
Impulse Bit	I_{bit}	=	4 mN-s
Efficiency	η_a	=	13.7%
Specific Impulse	I_{sp}	=	1160 s

Table 5: Summary of APPT module for Pluto Express Mission.

up of eight miniature APPT electrode sets with very small capacitors and electrodes. The electrical components are, in fact, so small that the fixed mass of the thruster dominates the mass of each module. For optimization purposes, the exhaust velocity was set near the PEP characteristic velocity, approximately 10 km/s, and the mass of the fuel was set according to the total impulse requirement. The maximum power used during pointing maneuvers is 2 W and the discharge energy is 87.3 mJ. The smallest impulse bit is 2.17 μN-s with a thrust of 40 μN. The electrode mass and ignition circuitry (if required) is scaled down to 0.25 kg per module. The total mass of the RCS system is 2.3 kg. A 5.0 kg contingency is included for redundancy in the total APPT system.

5.4 Total Design Overview and Comparison

Table 6 shows the proposed Pluto Express Spacecraft using APPT technology for both the main propulsion system and RCS. The total APPT propulsion

Mass Allocations:	(kg)	(frac)	(chg)
Power Subsystem	20.4	0.18	+6%
Structure	15.0	0.13	
Propulsion System	(13.9)	(0.12)	+33%
Main APPT	6.6	0.06	
RCS APPT Sys.	2.3	0.02	
Contingency	5.0	0.04	
Useful Mass:	(43.9)	(0.38)	+19%
Telecomm.	12.8	0.11	
Att. Cont.	6.6	0.06	
Space. Data	6.5	0.06	
Therm. Cont.	3.7	0.03	
Science Pay.	14.0	0.12	+100%
Dry Mass:	92.9	0.81	+14%
Contingency (20%)	18.6	0.16	+14%
Prop (ΔV=350 m/s)	3.5	0.03	-80%
Total Mass:	**115.0**	**1.00**	

Table 6: Proposed re-design of Pluto Express spacecraft.

system has approximately the same mass (without contingency) as the chemical system and uses only a slightly larger amount of power during operation. In other ways, this design is very similar to the 1993 design except that the propellant mass has been significantly reduced and the scientific payload mass has *doubled*.

6 Conclusions

The analysis for PEP system technology insertion into low power and small mass spacecraft is achieved by using universal scaling laws based on two characteristic velocities. The Langmuir and PEP characteristic velocities describe the size of the power generator and energy storage system with respect to the propellant mass. The Langmuir characteristic velocity has been used before for many general electric propulsion devices; pulsed systems require the PEP characteristic velocity to also be included in the analysis. Using these two velocities, or only one if it is much smaller than the other, allows an optimal exhaust velocity to be chosen that maximizes the useful mass fraction of the spacecraft.

Parameters based on technology that is available today have been used in this study to describe the relative size of these velocities and to demonstrate feasibility. Pulsed propulsion systems have proven to be beneficial and the PEP characteristic velocity is shown to be important when power levels are low, operation times are long, and the total mission ΔV is small. These missions include stationkeeping for large satellites, orbit raising for small satellites, and course correction maneuvers for small interplanetary probes.

The Pluto Express Mission is a good example where PEP system technology, specifically the APPT, can be optimized with the universal scaling laws and an advantage over conventional systems is realized. A 100% increase was shown in the scientific payload mass of a recent probe design using an APPT system made with off-the-shelf technology instead of a chemical based system. The new design for the APPT falls within the range of other, previously flight proven APPT systems, and could be made available for the Pluto Express Mission.

References

[1] D.B. Langmuir. Low-thrust flight: Constant exhaust velocity in field-free space. In H.S. Seifert, editor, *Space Technology*. John Wiley and Sons, Inc., 1959.

[2] E. Stuhlinger. *Ion propulsion for space flight*. McGraw-Hill, 1964.

[3] C.G. Sauer, Jr. Application of solar electric propulsion to future planetary missions. In *19th International Electric Propulsion Conference*, Colorado Springs, Colorado, May 11-13 1987. AIAA 87-1053.

[4] R.M. Myers. Electromagnetic propulsion for spacecraft. In *Aerospace Design Conference*, Irvine, California, February 16-19 1993. AIAA 93-1086.

[5] R.J. Vondra and K.I. Thomassen. A flight qualified pulsed plasma electric thruster for satellite control. In *AIAA 10th Electric Propulsion Conference*, Lake Tahoe, Nevada, October 31-November 2 1973. AIAA 73-1067.

[6] W.L. Ebert, S.J. Kowal, and R.F. Sloan. Operational Nova spacecraft teflon pulsed plasma thruster system. In *25th Joint Propulsion Conference*, Monterey, California, July 10-12 1989. AIAA 89-2497.

[7] A. Solbes and R.J. Vondra. Performance study of a solid fuel pulsed electric microthruster. In

9th Electric Propulsion Conference, Bethesda, Maryland, April 17-19 1972. AIAA 72-458.

[8] W.J. Guman. Designing solid propellant pulsed plasma thrusters. In *AIAA 11th Electric Propulsion Conference*, New Orleans, Louisiana, March 19-21 1975. AIAA 75-410.

[9] W.J. Guman, R.J. Vondra, and K.I. Thomassen. Pulsed plasma propulsion system studies. In *8th Electric Propulsion Conference*, Stanford, California, August 31-September 2 1970. AIAA 70-1148.

[10] N.N. Antropov, G.A. Popov, and A.I. Rudikov. Development and laboratory test of erosion pulsed plasma thruster, designed for the attitude control of a geostationary satellite. In *23rd International Electric Propulsion Conference*, Seattle, Washington, September 1993. IEPC 93-160.

[11] R.M. Myers. Low power pulsed MPD thruster system analysis and applications. In *29th Joint Propulsion Conference*, Monterey, California, June 28-30 1993. AIAA 93-2391.

[12] C.G. Sauer, Jr. Planetary mission performance for small solar electric propulsion spacecraft. In *Astrodynamics Conference*, Victoria, BC, Canada, August 16-19 1993. ASS 93-561.

[13] D.G. Feam. A mission to pluto using nuclear electric propulsion. In *23rd International Electric Propulsion Conference*, Seattle, Washington, September 1993. IEPC 93-200.

[14] R.J. Vondra. One millipound pulsed plasma thruster development. In *AIAA 16th International Electric Propulsion Conference*, New Orleans, Louisiana, November 17-19 1982. AIAA 82-1877.

[15] W.J. Guman. Solid propellant pulsed plasma micro-thruster studies. In *6th Aerospace Sciences Meeting*, New York, New York, January 22-24 1968. AIAA 68-85.

[16] D.J. Palumbo and W.J. Guman. Pulsed plasma propulsion technology. Interim Report AFRPL-TR-73-79, Air Force Rocket Propulsion Laboratory, May 1973.

[17] R. Dethlefsen and J. Ennis. Capacitors for pulsed electric propulsion. In *20th International Electric Propulsion Conference*, Garmisch-Partenkirchen, Germany, October 3-6 1988. IEPC 88-125.

[18] M.F. Rose. High energy density capacitors for space power conditioning. *IEEE AES Magazine*, pages 17–22, November 1989.

[19] J.B. Ennis, D.K. Haskell, and J.A. Sevigny. Development of energy storage/pulse discharge capacitors. In *34th International Power Sources Symposium*, Cherry Hill, New Jersey, June 25-28 1990.

[20] E.Y. Choueiri. A system optimization model for the application of ablative pulsed plasma thrusters to stationkeeping missions. In *30th Joint Propulsion Conference*, Indianapolis, Indiana, June 27-29 1994. AIAA 94-3392.

[21] D.J. Palumbo, M. Begun, and W.J. Guman. Pulsed plasma propulsion technology. Interim Report AFRPL-TR-74-50, Air Force Rocket Propulsion Laboratory, July 1974.

[22] D.J. Palumbo and W.J. Guman. Effects of propellant and electrode geometry on pulsed ablative plasma thruster performance. In *AIAA 11th Electric Propulsion Conference*, New Orleans, Louisiana, March 19-21 1975. AIAA 75-409.

[23] D.J. Palumbo. Solid propellant pulsed plasma propulsion system development for N-S stationkeeping. In *AIAA 14th International Electric Propulsion Conference*, Princeton, New Jersey, October 30-November 1 1979. AIAA 79-2097.

[24] P. Stella. Photovoltaic options for solar electric propulsion. In *21st International Electric Propulsion Conference*, Orlando, Florida, July 18-20 1990. AIAA-90-2529.

[25] K. Gledhill. Future trends in solar photovoltaics. In *29th Intersociety Energy Conversion Engineering Conference*, Monterey, California, August 7-11 1994. AIAA 94-3970.

[26] R.M. Myers and S.R. Oleson. Small satellite electric propulsion options. In *29th Intersociety Energy Conversion Engineering Conference*, Monterey, California, August 7-11 1994. AIAA 94-4137.

[27] R.L. Staehle et al. Exploration of pluto. *Acta Astronautica*, 30:289–310, 1993.

[28] R.L. Staehle et al. Last but not least–trip to pluto, parts 1 and 2. *Spaceflight*, 1994. 35:101-104 and 36:140-143.

[29] D.H. Morash and L. Strand. Miniature propulsion components for the pluto fast flyby spacecraft. In *30th Joint Propulsion Conference*, Indianapolis, Indiana, June 27-29 1994. AIAA 94-3374.

[30] A. Schock and C. Tak Or. Effect of fuel and design options on RTG performance versus PFF power demand. In *29th Intersociety Energy Conversion Engineering Conference*, Monterey, California, August 7-11 1994. AIAA 94-4128.

[31] A. Schock, C. Tak Or, and V. Kumar. Design modification for increasing the BOM and EOM power output and reducing the size and mass of RTG for the pluto mission. In *29th Intersociety Energy Conversion Engineering Conference*, Monterey, California, August 7-11 1994. AIAA 94-4129.

[32] W.R. Determan, D. Chung, A. Stadnik, and R.A. Johnson. Low power DIPS for interplanetary missions. In *25th Intersociety Energy Conversion Engineering Conference*, Reno, Nevada, August 12-17 1990.

[33] E.P. Chivington and T.L. Hershey. A solar heated AMTEC spacecraft power system. In *29th Intersociety Energy Conversion Engineering Conference*, Monterey, California, August 7-11 1994. AIAA 94-3814.

[34] A. Chmielewski. RTG's for space exploration at the end of the 20th century. In *24th Intersociety Energy Conversion Engineering Conference*, Washington, DC, August 6-11 1989. IECEC 899237.

[35] D.M. Rowe. Applications of nuclear-powered thermoelectric generators in space. *Applied Energy*, 40:241–271, 1991.

[36] G.L. Bennett, R. W. Campbell, R.J. Hemler, and L.R. Putnam. Status report on performance of radioisotope thermoelectric generators using silicon germanium thermoelectric elements. In *29th Intersociety Energy Conversion Engineering Conference*, Monterey, California, August 7-11 1994. AIAA 94-4127.

[37] R.F. Hartman. Modular RTG technology status. In *25th Intersociety Energy Conversion Engineering Conference*, Reno, Nevada, August 12-17 1990.